

Hybrid carbon nanotubes/graphene modified acrylic coats

Szymon Kugler, Krzysztof Kowalczyk*, Tadeusz Spychaj

West Pomeranian University of Technology in Szczecin, Polymer Institute, ul. Pułaskiego 10,
70-322 Szczecin, Poland

*Corresponding author. Tel. +48 91 449 4178; fax: +48 91 449 4247.

E-mail: kkowalczyk@zut.edu.pl

Abstract

Water-borne one-component acrylic coating compositions and coats modified with carbon nanotubes (CNTs), graphene (GN), as well as hybrid carbon nanofillers (CNT/GN mixture) have been prepared and evaluated. These coating materials were successfully formulated on a basis of commercial components, i.e. acrylic resin aqueous dispersion, CNT and/or GN and auxiliary agents. Influence of a kind and ratio of incorporated carbon nanofillers on the following properties was investigated: electrical surface resistivity, transparency, gloss, mechanical features (hardness and cross-cut adhesion) as well as on thermal properties (glass transition temperature, storage modulus and thermal stability) of coats. The presence of carbon nanostructure significantly improved electrical conductivity, hardness, storage modulus and thermal stability of the coats. Moreover, the nanofillers do not negatively influence adhesion and glass transition temperature.

Keywords: acrylic dispersion, nanocomposite, carbon nanotubes, graphene, electrical surface resistivity

1. Introduction

Polymeric coats modified with carbon nanofillers attract attention in the last decade. Decorative, protective as well as special features of coats, such as electrostatic discharge, high mechanical performance, broad range of operating temperature, anti-wear characteristics, chemical resistance and thermal conductivity are affected by an introduction of carbon nanotubes (CNTs), i.e. single-wall (SWCNT) or multi-wall type (MWCNT), as well as graphene (GN). Intrinsic properties of carbon nanofillers (CNs) applied to fill polymer films, i.e. high electrical conductivity and transparency (SWCNT, GN) or thermal conductivity (CNT, GN) allow to change the polymeric layers from insulating to conductive materials [1-6]. CNs modified coats can find a wide application in coating technology, mainly for electromagnetic shielding and anti-electrostatic coverings. Static charges can be built up as a result of electron transfer due to sliding of a material which is a prime generator of electrostatic voltage, e.g. plastics. Static control seeks to prevent a damage of material caused by a sudden discharge of that electrostatic potential from one body to another. Generally, with respect to electric surface resistivity features polymer-based coats can be divided into three categories: antistatic (10^{11} – 10^{14} Ω), static dissipative (10^5 – 10^{11} Ω) and conductive ($<10^5$ Ω) [7]. Another usable coat features can also be improved by CNTs or GN addition, e.g. corrosion resistance [8-11], UV resistance [9], mechanical [12], tribological [13,14] or hydrophobic properties [15,16]. There is available literature referring preparation and properties of CNs modified coats based on widely applied acrylic, polyurethane or epoxy resins cured by UV-initiated polymerization [1-4]. CNs modified coats applied on various substrates using spray [9,13], electro-deposition [10], doctor blade [11] or spin coating [17] techniques are also described. Majority of literature references for coating material formulations describe systems based on laboratory made CNT, GN and polymeric binders [3,4,8,10,11,13,18-20]. Only few announcements refer application of both commercial CNT

and GN in coating resins [1,2,9,12]. Water-borne coating systems are superior of the other, i.e. solvent-borne or UV-curable, in that respect they are applicable on the large scale and do not contain organic solvents. These reasons make them friendly from health and the environment viewpoints. While works on solvent-borne and solventless coating systems can be relatively often found in a literature, there are only few publications on conventional water-borne coating systems with CNs [18-20].

This work presents water-borne acrylic-based 1K coating compositions and coats based on commercial components, i.e. acrylic resin aqueous dispersion, MWCNTs, GN as well as auxiliary agents. MWCNTs and MWCNTs/GN hybrid mixtures were applied for aqueous acrylic varnish modifications and total content of CNs was kept in a range of 0.2–1.0 wt.%. Influence of a kind and ratio of incorporated CNs on coating properties were investigated. Electrical surface resistivity, transparency, gloss, thermal properties (glass transition temperature, storage modulus and thermal stability) as well as mechanical features (hardness and cross-cut adhesion to glass substrate) were evaluated.

2. Experimental

2.1. Materials

The following materials were used:

- commercial aqueous acrylic dispersion, 45 wt.% of solids, viscosity 70 mPa·s (Mowilith Nano 9420, Celanese Emulsions GmbH, Germany);
- aqueous dispersion of commercial NC7000 multi-walled carbon nanotubes (IP-CNT, 2 wt.% of MWCNT), with average length of 1.5 μm , average diameter of 9,5 nm, average specific surface 275 m^2/g (Nanocyl, Belgium); dispersion was prepared in our laboratory via sonication;
- aqueous dispersion of commercially available graphene (IP-GN, 1 wt.% of GN), with specific surface $>750 \text{ m}^2/\text{g}$, particle diameter of less than 0.1 μm and less than 3 carbon

layers (Graphene Technologies, USA); dispersion was prepared in our laboratory via sonication;

- commercial silicone auxiliary additive for aqueous coating systems (BYK-094, BYK-Chemie, Germany).

2.2. Sample preparation

Acrylic varnishes with carbon nanofillers were prepared as follows: firstly the aqueous acrylic dispersion was mixed with BYK-094 (0.5 wt.% of coating composition) by mechanical stirring (300 rpm, 15 min). Next, the stirring speed was increased to 600 rpm and the proper amount of carbon nanofiller aqueous dispersion(s) (IP-CNT and/or IP-GN) was added. The composition was additionally mixed for 30 min. Prepared varnish was applied onto a glass and poly(ethylene terephthalate) (PET) substrate by means of gap applicator (Zafil, Poland) and dried for 48 h at room temperature in order to obtain a coat with thickness of 40 μm . The composition and sample acronyms are compiled in Table 1.

2.3. Methods

Viscosity of coating compositions was evaluated using high shear viscometer (I.C.I. cone-plate system, Research Equipment Ltd, UK). Electrical surface resistivity of dry coats (glass substrate, 20°C, 50 % of RH) was determined according to the standard PN-E-04405 (10 V) using electrometer 6517A with electrode set Keithley 8009 (Keithley Instruments, Inc.).

Transmission Electron Microscopy was performed using JEM 1200EX instrument (Jeol, Japan). Transparency of dry coats on a PET foil was measured by UV-Vis spectroscopy (V-630 spectrophotometer, Jasco Inc, USA). The pendulum hardness of dry coats on a glass substrate was tested according to the standard PN-EN ISO 1522 using König pendulum (AWS-5, Dozafil, Poland); five measurements of each sample were carried out. Gloss at 20° was determined using Rhopoint IQ206085 device (Rhopoint Instruments, UK) in compliance with the ISO 2813 standard (three measurements of each sample were performed). Adhesion

of dry coats to glass substrate was tested according to the standard PN-EN ISO 2409 (cross-cut method, three tests of each sample were carried out). Glass transition temperatures (T_g) of coats were evaluated by Differential Scanning Calorimetry (DSC) and Dynamic Mechanical Analysis (DMA) methods. DSC analysis was performed on small sample (ca. 10 mg) of dried nanocomposite coats; hermetic Al pans were used with scanning range -20 – 180°C and heating rate of $5^\circ\text{C}/\text{min}$. DSC Q100 device (TA Instruments, USA) was used. DMA tests were taken in the following conditions: tension test in a range of 0 – 140°C , heating rate $3^\circ\text{C}/\text{min}$, 1 Hz of frequency, amplitude $15\ \mu\text{m}$. DMA Q800 analyser (TA Instruments) was used. The T_g values of samples on a basis of tan delta peak temperature were determined. Thermogravimetric Analysis (TGA) was made using Q5000 thermoanalyzer (TA Instruments). Small doses (ca. 10 mg) of dried coats were examined in an air atmosphere. Temperature range was 20 – 600°C with heating rate of $10^\circ\text{C}/\text{min}$. Surface roughness (R_z parameter), i.e. distance between the deepest valley and the highest peak of a coat surface was investigated (ten measurements of each sample) using laser scanning microscope VK-9700 (Keyence, USA).

3. Results and discussion

3.1. Viscosity of coating compositions

The viscosity test results of water-borne acrylic coating compositions are presented in Table 1. The viscosity values were in the range of 10 – $70\ \text{mPa}\cdot\text{s}$. The viscosity decreased with increasing amount of IP-CNT dispersion from $70\ \text{mPa}\cdot\text{s}$ (RS-0) to $20\ \text{mPa}\cdot\text{s}$ (CNT-0.6, CNT-0.8, CNT-1). Moreover, the increasing amount of IP-GN dispersion caused deeper decrease of varnish viscosity ($10\ \text{mPa}\cdot\text{s}$ for CNT/GN-0.2/0.8 and GN-1). Such figure is obvious if one takes into account that carbon nanofillers aqueous dispersions contained much more water ($>90\ \text{wt.}\%$) than basic acrylic dispersion ($45\ \text{wt.}\%$) and, moreover, IP-GN ($1\ \text{wt.}\%$ of GN) contained more water than IP-CNT ($2\ \text{wt.}\%$ of CNT).

3.2. Electrical properties of the coats

The influence of CNT, CNT/GN or GN nanofillers on electrical surface resistivity of coats is presented in Fig. 1. In general the addition of CNT strongly decreased the mentioned parameter value of acrylic systems and the percolation threshold was observed at 0.4–0.5 wt.% content of carbon nanotubes. Samples containing 0.5–1 wt.% of CNT exhibited significant static dissipative properties. Coat with 1 wt.% of CNT (CNT-1) was characterized by surface resistivity lowered by 9 orders of magnitude ($1.8 \cdot 10^5 \Omega$) in comparison with the reference sample (RS-0; $1.0 \cdot 10^{14} \Omega$). On the other hand, surface resistivity of GN modified coats proved to be relatively high (over $1 \cdot 10^{13} \Omega$). Although the replacement of a part of graphene by a relevant part of CNTs in acrylic coat (to a total amount of 1 wt.% of CNs) reduced that electrical parameter in higher degree as it could be expected from simple addition rule. This effect was particularly observable for CNT/GN samples with at least 0.4 wt.% content of nanotubes (i.e. CNT/GN-0.4/0.6, CNT/GN-0.5/0.5, CNT/GN-0.6/0.4 and CNT/GN-0.8/0.2), which showed reduced surface resistivity values between $9.5 \cdot 10^7 \Omega$ and $3.3 \cdot 10^5 \Omega$, respectively. Comparison of coats with the same CNT content (CNT/GN-0.4/0.6 and CNT-0.6, CNT/GN-0.5/0.5 and CNT-0.5 etc.) shows that GN profitably influenced on the reduction of coat resistivity, e.g. from $5.3 \cdot 10^{12} \Omega$ (CNT-0.4) to $9.5 \cdot 10^7 \Omega$ (CNT/GN-0.4/0.6). Although graphene decreased surface resistivity of CNT modified acrylic coats, that impact is considerably smaller than in the case of CNT addition (Fig. 1). It probably resulted from the shape of CNT and GN fillers. Strongly elongated CNT can easily form electroconductive nanostructure/web in polymeric matrix (Figs 1A). On the other side, GN in coat is separated into single platelets/small packets (sample with low electrical conductivity; Fig. 1B) while in the case of CNT addition (and proper CNT/GN ratio) these GN particles act as “electrical switchboards” improving current flow through the nanocomposite material. Furthermore, graphene particle exhibits generally higher electrical conductivity than multiwalled carbon nanotube, however that parameter value is much higher for compressed CNT than GN

powder. A simple explanation of that phenomenon is quite a number of contact points between adjacent nanotubes [21]. Due to the initial form of tested coating material, i.e. aqueous dispersion, a compression of the CN between polymeric particles occurs during coat drying (water evaporation) and coalescence process. Thus coats with CNT exhibit generally higher electrical conductivity than samples with GN only. Nevertheless, the volumetric content of CN in coat influences on its electrical conductivity as well [5,21].

According to our knowledge, no one has investigated the electrical surface resistivity of coats based on water-borne polymeric dispersions, nevertheless some results for UV-cured [1,2], as well as solvent-borne [15,16] and solventless [22] thermally cured coats have been described. Ha and coworkers prepared coats with 0.1 wt.% of CNT and surface resistivity ca. $4 \cdot 10^6 \Omega$ [1], while Sangermano et al. obtained UV-cured coats (1 wt.% graphene oxide) exhibiting $5 \cdot 10^6 \Omega$ [2]. On the other hand, Liu et al. [16] noted $4.2 \cdot 10^{10} \Omega$ for coat with 1 wt.% of CNT, whereas Jeong et al. [22] prepared solventless thermally cured films characterized by electrical resistance of ca. $3 \cdot 10^3 \Omega$ (coat with 5 wt.% content of CNT/GN mixture in a weight ratio 1:1). The comparison of surface resistivity of investigated acrylic coats (from water-borne system) with results achieved by the mentioned research teams are presented in Fig. 2. Taking into consideration that the analyzed acrylic coats modified with CNT or CNT/GN were solely composed using commercial components, recorded electrical properties are satisfactory.

3.3. Functional and mechanical properties of the coats

Although CNT improved electrical conductivity of the coats, it also affected their optical feature. The results of transparency evaluation of 40 μm thick acrylic coats with CNs on PET foil are graphically presented in Figs 3A and 3B. The addition of CNT decreased that parameter to the range from 54 % (CNT-0.2) to 18 % (CNT-1). On the other hand, coats with 1 wt.% of GN or CNT/GN exhibited significantly higher transparency (Fig. 3B) than coat

with 1 wt.% of CNT (CNT-1; Fig. 3A). The sample containing 1 wt.% of GN (GN-1) showed 45 % of transmittance while evaluated coats with CNT/GN were between 33 % (CNT/GN-02/08) and 20 % (CNT/GN-08/02). Therefore, in the investigated coating systems GN filler exceeded the CNT in term of transparency, which was in accordance with available data for UV-curable systems with these CNs [1,2]. Although transparencies of thermally cured solvent-borne [16] and UV-cured [1,2] coats on glass or PET substrates were described in the literature, their thicknesses were not reported, so current results cannot be compared to them. The beneficial impact of GN on the transparency of investigated acrylic coats was accompanied by improvement of their hardness (Fig. 4A). As can be seen, the hardness of reference coat without CNs (RS-0) reached 48 units and did not increase after CNT addition (47 units for CNT-1). On the other hand, GN improved that feature (55 units for GN-0.5, up to 73 units for GN-1). The most significant improvement of the CNT/GN modified coats hardness was noted for samples with GN content above 0.5 wt.%, (i.e. 52 units for CNT/GN-0.5/0.5 and 64 units for CNT/GN-0.1/0.9). Thus the dominant presence of GN in carbon nanofillers mixture improved the hardness of tested coats, in contrast to the CNT, which did not modify that parameter; it is generally known, that platelet-like nanoparticles (eg. modified aluminosilicate) increase hardness of coating materials [23].

Almost all investigated coats showed good adhesion evaluated by cross-cut method. The values of that parameter are presented in Table 1, the rating scale was from 0° (perfect adhesion, no delamination occurred) to 5° (weak adhesion, over 65 % of coat area removed). Only CNT/GN-08/02 coat reached 1° (i.e. less than 5 % of surface delamination). Generally, the cross-cut test results show that the presence of either CNT or GN did not negatively impact on the coats adhesion.

Gloss of prepared coats strongly depended both on the content and the type of CN (Fig. 4B). Gloss of reference coat was ca. 139 gloss units (G.U.) and the addition of CNT decreased its

values to the range from 90 G.U. (CNT-0.2) to 60 G.U. (CNT-1). With the increase of GN content (instead CNT) the gloss of coats was further decreased from 52 G.U. (CNT/GN-0.8/0.2) to 27 G.U. (CNT/GN-0.2/0.8), with a slight increase for GN-1 sample (G.U.). Thus GN affected the coats gloss noticeably more than CNT.

Interestingly, CNs influenced on thermomechanical features of dry acrylic films. Fig. 5 presents storage moduli changes for samples with 1 wt.% of CNs. The analyzed parameter value for reference sample (~~RS-0~~) was 3.8 GPa (20°C), while carbon filled films exhibited 4 GPa (CNT-1), 4.5 GPa (GN-1) and 5 GPa (CNT/GN-0.5/0.5). It can be seen that sample with 1 wt.% of GN reached significantly higher storage modulus than a film with similar content of CNT (~~1 wt.%)~~ and, moreover, CNT/GN mixture increased much more the storage modulus in comparison with either GN or CNT. It should be mentioned that observed increment of storage modulus for samples with GN (ca. +0.7 GPa in relation to reference sample) was markedly higher than referred in the literature [12,18].

3.4. Thermal properties of the coats

The glass transition temperature (T_g) values of investigated coats evaluated by DSC and DMA techniques are presented in Table 1. Taking into consideration the DSC results, a presence of either CNT or GN did not significantly affect the analyzed parameter of dry coats; T_g values for RS-0 and CNs modified coats were in a narrow range of 13.1–13.4°C. The range of T_g determined by DMA was slightly broader (10.7–13.5°C), however, evident influence of CNs content on the analyzed parameter value was not observed (as it was reported by the others [20,24]). The maximum T_g for CNT modified coats was 13.5°C (CNT-0.6), whereas for samples with CNT/GN nanofiller reached 11.6°C (CNT/GN-0.6/0.4 and CNT/GN-0.8/0.2). The differences between DSC and DMTA results were observed due to various mechanisms of T_g determination by these both techniques. Whereas DSC measures the specific heat change for material during transition from the glassy to the rubber state, DMA determines its

viscoelastic characteristics, i.e. loss and storage moduli, tan delta loss factor). Therefore transition temperature determined by DMA is based on a kinetic phenomenon as opposed to temperature specified by DSC, which reflects a phenomenon of an equilibrium character. Consequently, a variation of T_g values determined by DSC and DMA (storage modulus) can reach even 15°C [25]. It is noteworthy that in scientific literature the DMA technique was used for T_g analysis of CN modified nanocomposites [3,12] rather than DSC, which was utilized for other phase transitions [12] or crosslinking reactions [1] evaluation.

Thermal stability of acrylic coats evaluated by TGA, i.e. temperatures at 10 % mass loss (T_{10}) is presented in Fig. 6. As can be seen, the CNs addition considerably enhanced T_{10} value of the coats during heating under air, however, the influence of CNT on discussed value is significantly stronger than of GN. The T_{10} value for reference sample (RS-0) was 309°C, while the GN addition caused linear increment of the value up to 325°C (GN-1). On the other hand, the CNT incorporation in amounts of 0.2–0.3 wt.% increased T_{10} to 327°C (CNT-0.2) and to 340°C (CNT-0.3). The further increase of CNT content (0.4–1.0 wt.%) did not enhance the T_{10} value, which remained at the level of 340°C. Intriguingly, an influence of CNT/GN mixture addition on T_{10} value of dry coats was not linear, but showed a peak (CNT/GN-0.2/0.8 and CNT/GN-0.3/0.7) and a valley (CNT/GN-0.4/0.6, CNT/GN-0.5/0.5 and CNT/GN-0.6/0.4). This phenomenon has not been described in a literature. Nevertheless, the TGA results were in accordance with the surface roughness assessment. The roughness of dry coats directly depended on type and content of CNs and it reached 0.1 μm (RS-0), 0.15–0.17 μm (CNT-0.5, CNT-1) and 0.2–0.27 μm in the case of samples with GN (Fig. 7A). After heating of coats (300°C, 0.5 h) the R_z parameter markedly increased and the highest values were recorded for reference sample (2.42 μm) and for coats filled with GN (Fig. 7B). On the other hand, the smallest surface defects were observed for samples with CNT (ca. 1.9 μm for CNT-0.5 and CNT-1). Considering the presented results of R_z and T_{10} measurements it could be

claimed that CN, especially CNT, mechanically reinforced acrylic matrix and prevented/limited the thermal cracks formation in the coat during heating (these thermal defects were created in RS-0 during heating and it resulted in an increment of the surface roughness of the coat). In the case of thermal crack presence mass transport to the coat surface (during heating) was easier, thus higher mass loss was observed (i.e. lower T_{10} values). Figs 8A-M present the scheme of an influence of CNs on thermal stability of acrylic coat. Generally, RS-0 sample was unmodified by means of CNs (Figs 8A and 8B) and easily broke during heating; a heat transfer area was relatively large, so the thermal stability (T_{10}) was limited. The addition of GN particles (Figs 8C and 8D) limited the breaking process, thus the thermal stability rose. An introduction of a small amount of CNT (instead of GN; Figs 8E and 8F) markedly more enhanced thermal stability of coat, because elongated shape of CNT particles resulted in more effective mechanical reinforcement of the coat structure and prevention of its breaking (the peak in T_{10} distribution; Fig. 6). In the case of higher CNT addition (CNT/GN-0.5/0.5; Figs 8G and 8H) continuous thermal conductive CNT-GN structure was created and heat transfer throughout the coat was increased (thermal degradation process of polymeric matrix was more productive and the T_{10} value has been reduced in relation to the coat with lower CNT/higher GN content). That phenomenon was not observed for samples with higher GN content. Although GN exhibits significantly higher thermal conductivity than CNT, the continuous GN-GN structure was not created in the samples mainly based on that type of carbon nanofiller (Fig. 1B). It should be noted that polymeric nanocomposites (filled with CNT/GN mixture) exhibiting higher thermal conductivity than samples with either CNT or GN were described in the literature [26]. In the case of CNT/GN-type samples containing >0.5 wt. % of CNT improved thermal stability was recorded (the second peak at T_{10} curve for CNT/GN coats; Fig. 6). Nevertheless, it should be noted that low thermal stability of CNT/GN-0.5/0.5 could be caused by thermal crack

formation between adjacent GN and CNT particles. As can be observed in Fig. 1, this sample exhibited significantly higher electrical conductivity than coat with lower CNT/higher GN content (CNT/GN-0.4/0.6). It confirmed that continuous hybrid CNT-GN structure was created in acrylic coat containing the equal doses of both type of CNs; CNT-based bridges between GN particles was observed in thermal and electrical conductive polymeric materials [26].

Probably, improved thermal stability of CNT/GN-0.7/0.3, CNT/GN-0.8/0.3 and CNT-1 was caused by high CNT content (mechanical reinforcement effect and limited thermal crack formation) and/or lower GN content (reduced thermal conductivity of nanocomposites) in comparison with CNT/GN-0.5/0.5 composition. In the case of lower GN weight content in a sample, the CNT-GN contact was limited and thermal failure at the boundary of these CN particles was not occurred (Figs 8J and 8K). Finally, the highest thermal stability of CNT-1 coat was caused by a presence of stranded CNT structure in that sample (Figs 8L and 8M); formation of thermal crack in coat during heating was reduced, thus CNT-1 exhibited the lowest R_z value in relation to samples with GN or CNT/GN mixture.

A few thesis explaining positive influence of CNT on thermal stability of polymeric materials were described in a literature. These nanofillers can increase the viscosity of melted polymeric matrix (during heating) thus emission of gaseous product generated during thermal degradation of organic binder is limited. On the other hand, CNT addition into polymeric materials resulted in porous coke layer formation on a surface of heated sample. The mentioned coke exhibits high thermal barrier features and effectively protect the polymeric base [27]. Nevertheless, these theories are not useful to analysis of an influence of CNT addition on T_{10} value of the presented nanocomposite acrylic coatings. It should be noted that the coke layer was not observed during cross-section investigation of unfilled coats and coats with GN (i.e. CNT, GN or CNT/GN mixture) by means of LSM (results not presented).

Moreover, the shape of RS-0 and GN-based samples (free film) was not changed during heating at 300°C; it means that the melting process of acrylic matrix didn't occur during thermal stability test.

4. Conclusions

Water-borne acrylic coating compositions and coats with CNT and hybrid CNT/GN nanofillers were prepared and their properties evaluated. The surface resistivity values of these materials (mainly containing CNT/GN mixture) allow to apply them as novel transparent and static dissipative/electroconductive coats for various substrates (e.g. glass, plastics). The content of CNs at percolation threshold (≤ 1 wt.%) was significantly lower than in the case of polymeric materials filled with conventional electroconductive additives (powdered metals, metal oxides, carbon black or coated mica). Thus, widely known problems of high viscosity of coating compositions and brittleness of dry electroconductive coats [28,29] were avoided. Moreover, it should be noted that prepared water-borne coating systems entirely fulfill the environmental protection requirements on emission of volatile organic compounds.

Taking into account that commercial substrates were used for investigated samples preparation, the electrical properties of the coats are highly satisfactory. Although the surface resistivity values for coats with hybrid nanofillers were higher than for CNT modified samples, the usage of CNT/GN mixture increased the coats transparency in comparison to the samples with relevant amount of CNT. The presence of hybrid CNT/GN fillers in coat significantly improved its hardness and storage modulus. On the other hand, the CNs did not negatively influence on adhesion and glass transition temperature of dry acrylic coat and, moreover, distinctly improve its thermal stability.

Acknowledgements

This work was partly financially supported by European Research Agency (FP7-SME-2011 285908 “TransCond”).

Some of the results were presented as a poster at NanoTechItaly 2013 scientific conference (27–29.11.2013, Venice, Italy)

References

- [1] H. Ha, S.C. Kim, K.R. Ha, *Macromol. Res.* 18 (2010) 674-679. DOI: 10.1007/s13233-010-0705-8
- [2] M. Sangermano, S. Marchi, L. Valentini, S. Bittolo-Bon, P. Fabbri, *Macromol. Mater. Eng.* 296 (2011) 401-407. DOI: 10.1002/mame.201000372
- [3] M. Martin-Gallego, M. Hernandez, V. Lorenzo, R. Vardejo, M.A. Lopez-Manchado, M. Sangermano, *Polymer* 53 (2012) 1831-1838. DOI: 10.1016/j.polymer.2012.02.054
- [4] P. Fabbri, L. Valentini, S. Bittolo-Bon, D. Foix, L. Pasquali, M. Montecchi, M. Sangermano, *Polymer* 53 (2012) 6039-6044. DOI: 10.1016/j.polymer.2012.10.045
- [5] L. Chu, Q. Xue, J. Sun, F. Xia, W. Xing, D. Xia, et al., *Compos. Sci. Technol.* 86 (2013) 70–75. DOI:10.1016/j.compscitech.2013.07.001
- [6] Q. Li, Q. Xue, L. Hao, X. Gao, Q. Zheng, *Compos. Sci. Technol.* 68 (2008) 2290–2296. DOI:10.1016/j.compscitech.2008.04.019
- [7] M. Berkei, *CHEManager Europe* 7-8 (2011) 10.
www.chemanager-online.com/en/magazine/chemanager-europe-7-82011
- [8] L. Romo, R. Cruz-Silva, S. Sepulveda-Guzman, C. Menchaca, J. Uruchurtu, *ECS Transactions* 36(1) (2011) 111-118. DOI: 10.1149/1.3660604
- [9] N. Nuraje, S.I. Khan, H. Misak, R. Asmatulu, *ISRN Polym. Sci.* (2013) 514617, 8 pp. DOI: 10.1155/2013/514617
- [10] B.P. Singh, B. Kumar Jena, S. Bhattacharjee, L. Besra, *Surf. Coat. Technol.* 232 (2013) 475-481. DOI: 10.1016/j.surfcoat.2013.06.004
- [11] Y. Show, T. Nakashima, Y. Fukami, *J. Nanomaterials* (2013) 378752, 7 pp. DOI: 10.1155/2013/378752
- [12] D. Cai, K. Yusoh, M. Song, *Nanotechnology* 8 (2009) 085712, 5 pp. DOI: 10.1088/0957-4484/20/8/085712

- [13] H.J. Song, Z.Z. Zhang, X.H. Men, *Europ. Polym. J.* 43 (2007) 4092-4102. DOI:
10.1016/j.eurpolymj.2007.07.003
- [14] B. Pan, G. Xu, B. Zhang, X. Ma, H. Li, Y. Zhang, *Polymer-Plastics Technol. Eng.* 51
(2012) 1163-1166. DOI: 10.1080/03602559.2012.689052
- [15] M. Peng, J. Qi, Z. Zhou, Z. Liao, Z. Zhu, H. Guo, *Langmuir* 26 (2010) 13062-13064.
DOI: 10.1021/la102350t
- [16] J. Liu, R. Liu, Y. Yuan, S. Zhang, X. Liu, *Prog. Org. Coat.* 76 (2013) 1251-1257. DOI:
10.1016/j.porgcoat.2013.03.022
- [17] Z.A. Ghaleb, M. Martini, Z.M. Ariff, *Compos. Part A* 58 (2014) 77-83. DOI:
10.1016/j.compositesa.2013.12.002
- [18] X. Wang, W. Xing, L. Song, H. Yang, Y. Hu, G.H. Yuoh, *Surf. Coat. Technol.* 206
(2012) 4778-4784. DOI: 10.1016/j.surfcoat.2012.03.077
- [19] P. Vandervorst, C.H. Lei, Y. Lin, O. Dupont, A.B. Dalton, Y.-P. Sun, J.L. Keddie, *Prog.
Org. Coat.* 57 (2006) 92-97. DOI: 10.1016/j.porgcoat.2006.07.005
- [20] T.G. Gopakumar, N.S. Patel, M. Xanthos, *Polym. Compos.* 27 (2006) 368-380. DOI:
10.1002/pc.20199
- [21] B. Marinho, M. Ghislandi, E. Tkalya, C.E. Koning, G. de With, *Powder Technol.* 221
(2012) 351-358. DOI:10.1016/j.powtec.2012.01.024.
- [22] Y.G. Jeong, J.E. An, *Compos. Part A* 56 (2014) 1-7. DOI:
10.1016/j.compositesa.2013.09.003
- [23] K. Kowalczyk, T. Szychaj, *Prog. Org. Coat.* 62 (2008) 425-429
DOI:10.1016/j.porgcoat.2008.03.001
- [24] K. Kowalczyk, S. Kugler, T. Szychaj, *Polymers (Warsaw)* 59 (2014) 650-655. DOI:
10.14314/polimery.2014.650

[25] Dynamic Mechanical Analysis, Perkin-Elmer booklet.

www.perkinelmer.com/CMSResources/Images/44-74546GDE_IntroductionToDMA.pdf

(date of access: 4.07.2014)

[26] A. Yu, P. Ramesh, X. Sun, E. Bekyarova, M.E. Itkis, R.C. Haddon, *Adv. Mater.* 20 (2008) 4740-4744. DOI: 10.1012/adma.200800401

[27] B. Jurkowski, H. Rydarowski (eds.), *Materiały polimerowe o obniżonej palności* (Polymeric materials with reduced combustibility), ITE, Radom, 2012

[28] Z. Chen, Y. Tang, F. Yu, *J. Chin. Soc. Corros. Prot.* 29 (2009) 113–118. DOI:
<http://www.jcscp.org/CN/article/downloadArticleFile.do?attachType=PDF&id=8705>

[29] T. Gurunathan, C.R.K. Rao, R. Narayan, K.V.S.N. Raju, *J. Mater. Sci.* 48 (2013) 67–80.
DOI:10.1007/s10853-012-6658-x.

TABLE(S)

Hybrid carbon nanotubes/graphene modified acrylic coats

Szymon Kugler, Krzysztof Kowalczyk*, Tadeusz Spychaj

West Pomeranian University of Technology in Szczecin, Polymer Institute, ul. Pułaskiego 10,
 70-322 Szczecin, Poland

* Corresponding author. Tel. +48 91 449 4178; fax: +48 91 449 4247

E-mail: kkowalczyk@zut.edu.pl

Table 1. Properties of acrylic coating compositions and coats with carbon nanofillers

Sample acronym	CNT content ^a	GN content ^a	Viscosity (mPa·s)	Cross-cut adhesion ^b (°)	T _g (°C)	
					DSC	DMA
RS-0	0	0	70	0	13.3	10.7
CNT-0.2	0.2	0	30	0	13.1	— ^c
CNT-0.3	0.3	0	30	0	13.4	— ^c
CNT-0.4	0.4	0	25	0	13.2	11.3
CNT-0.5	0.5	0	25	0	13.2	11.6
CNT-0.6	0.6	0	20	0	13.1	13.5
CNT-0.8	0.8	0	20	0	13.4	11.0
CNT-1	1	0	20	0	13.3	11.5
CNT/GN-0.9/0.1	0.9	0.1	20	0	13.4	— ^c
CNT/GN-0.8/0.2	0.8	0.2	20	1	13.2	11.6
CNT/GN-0.6/0.4	0.6	0.4	15	0	13.3	11.6
CNT/GN-0.5/0.5	0.5	0.5	15	0	13.1	11.2
CNT/GN-0.4/0.6	0.4	0.6	15	0	13.1	11.3
CNT/GN-0.3/0.7	0.3	0.7	15	0	13.1	11.4
CNT/GN-0.2/0.8	0.2	0.8	10	0	13.1	11.3
CNT/GN-0.1/0.9	0.1	0.9	10	0	13.3	— ^c
GN-1	0	1	10	0	13.1	10.9
GN-0.8	0	0.8	15	0	13.4	— ^c
GN-0.5	0	0.5	20	0	13.2	— ^c

a – wt.%; b – rating scale 0° - 5° (0° – the best, 5° – the worst); c – not analyzed

FIGURE(S)

Hybrid carbon nanotubes/graphene modified acrylic coats

Szymon Kugler, Krzysztof Kowalczyk *, Tadeusz Spychaj

West Pomeranian University of Technology in Szczecin, Polymer Institute, ul. Pułaskiego 10,
70-322 Szczecin, Poland

* Corresponding author. Tel. +48 91 449 4178; fax: +48 91 449 4247

E-mail: kkowalczyk@zut.edu.pl

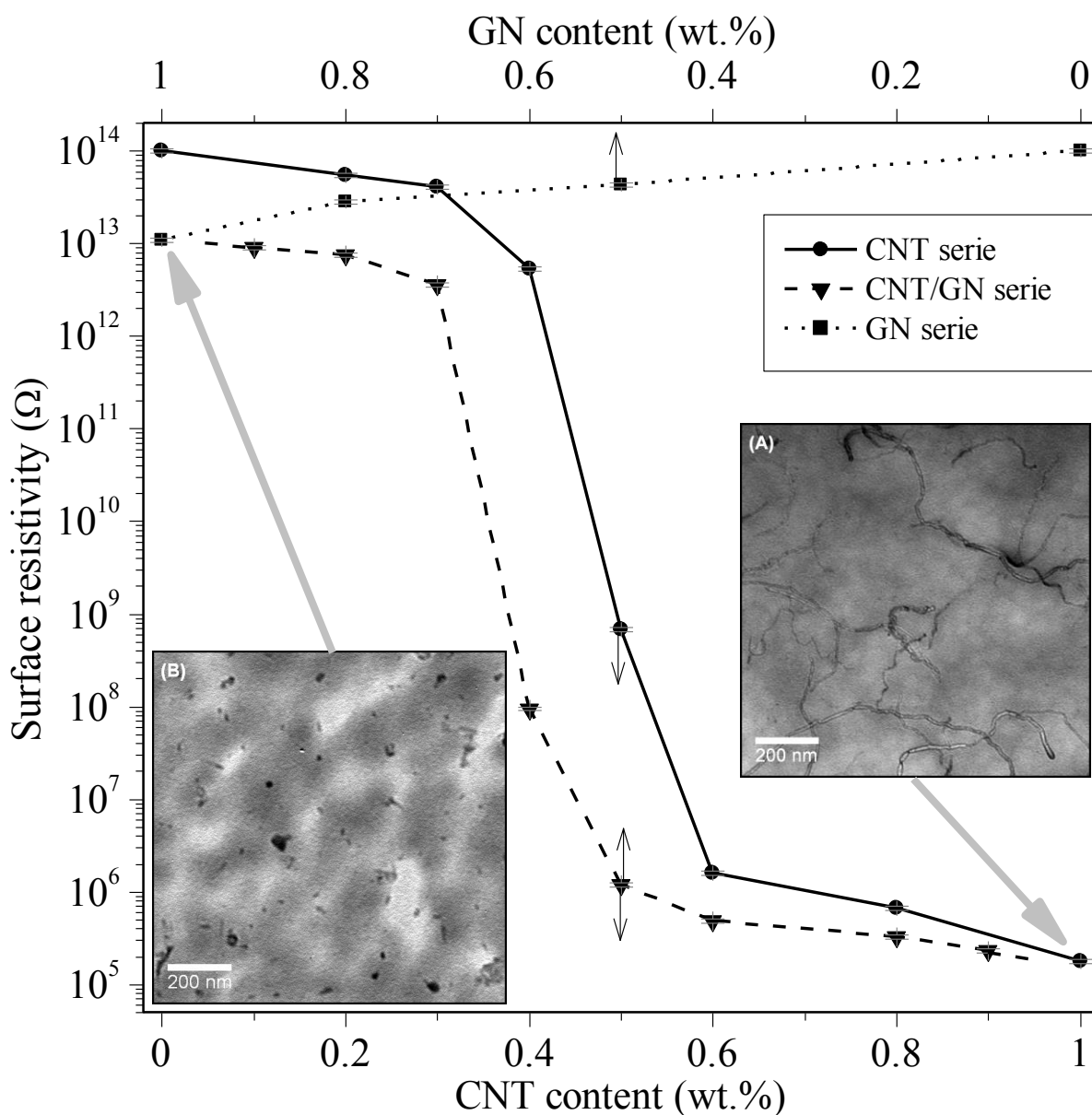


Fig. 1. Electrical surface resistivity of acrylic coats with carbon nanofillers and TEM images of (A) CNT-1 and (B) GN-1 samples

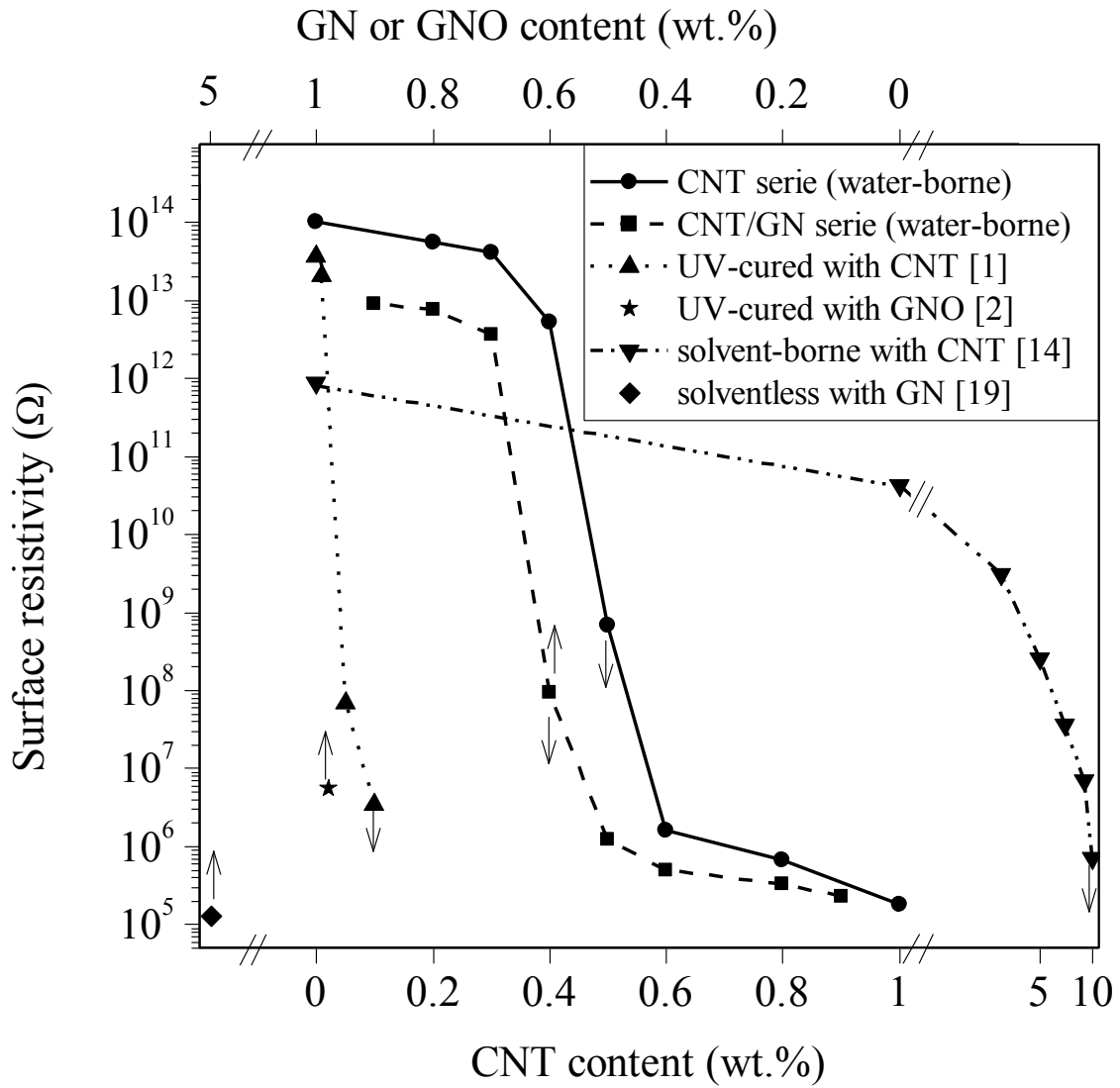


Fig. 2. Electrical surface resistivity results for different coating systems

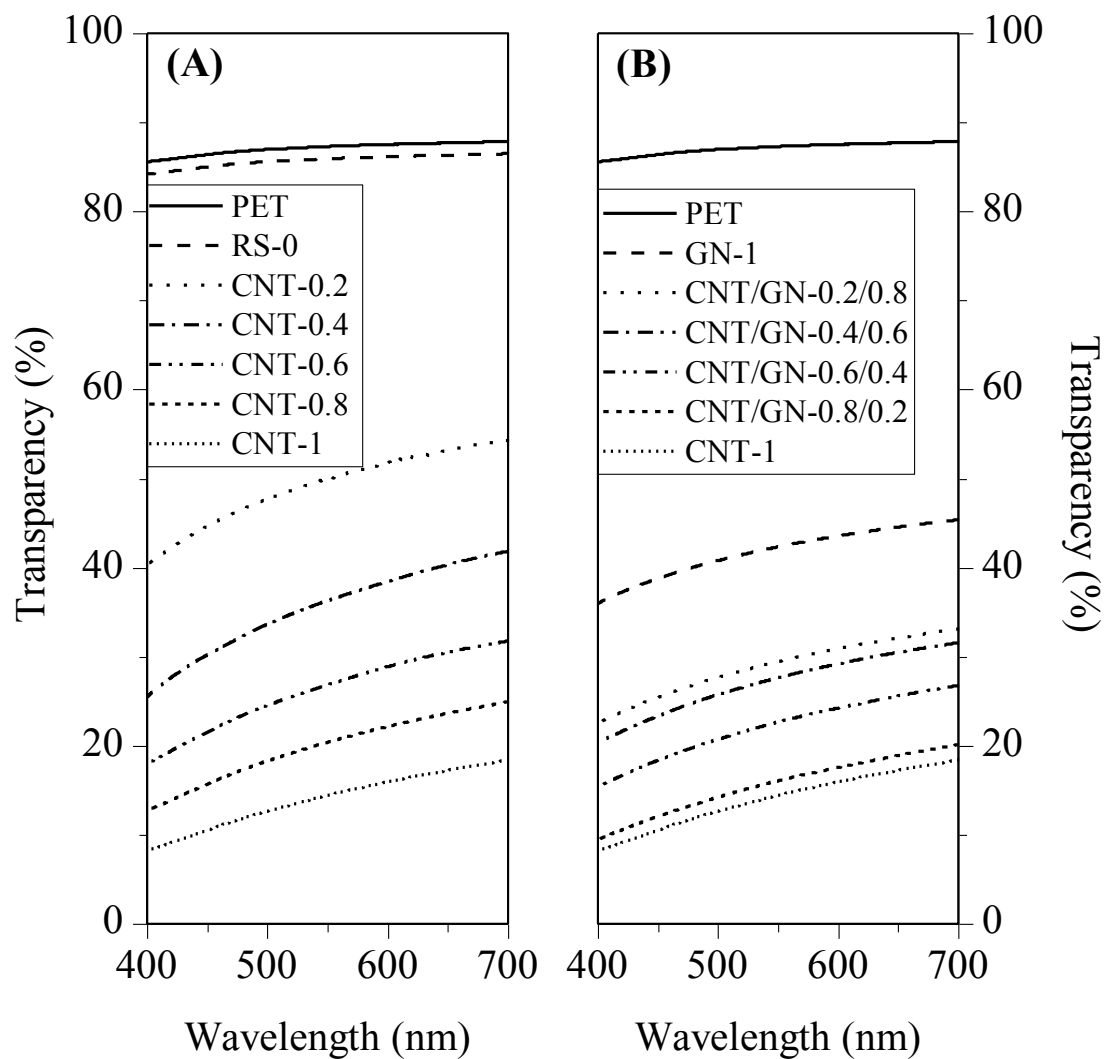


Fig. 3. Transparency of the acrylic coats with (A) CNT and (B) CNT/GN mixture

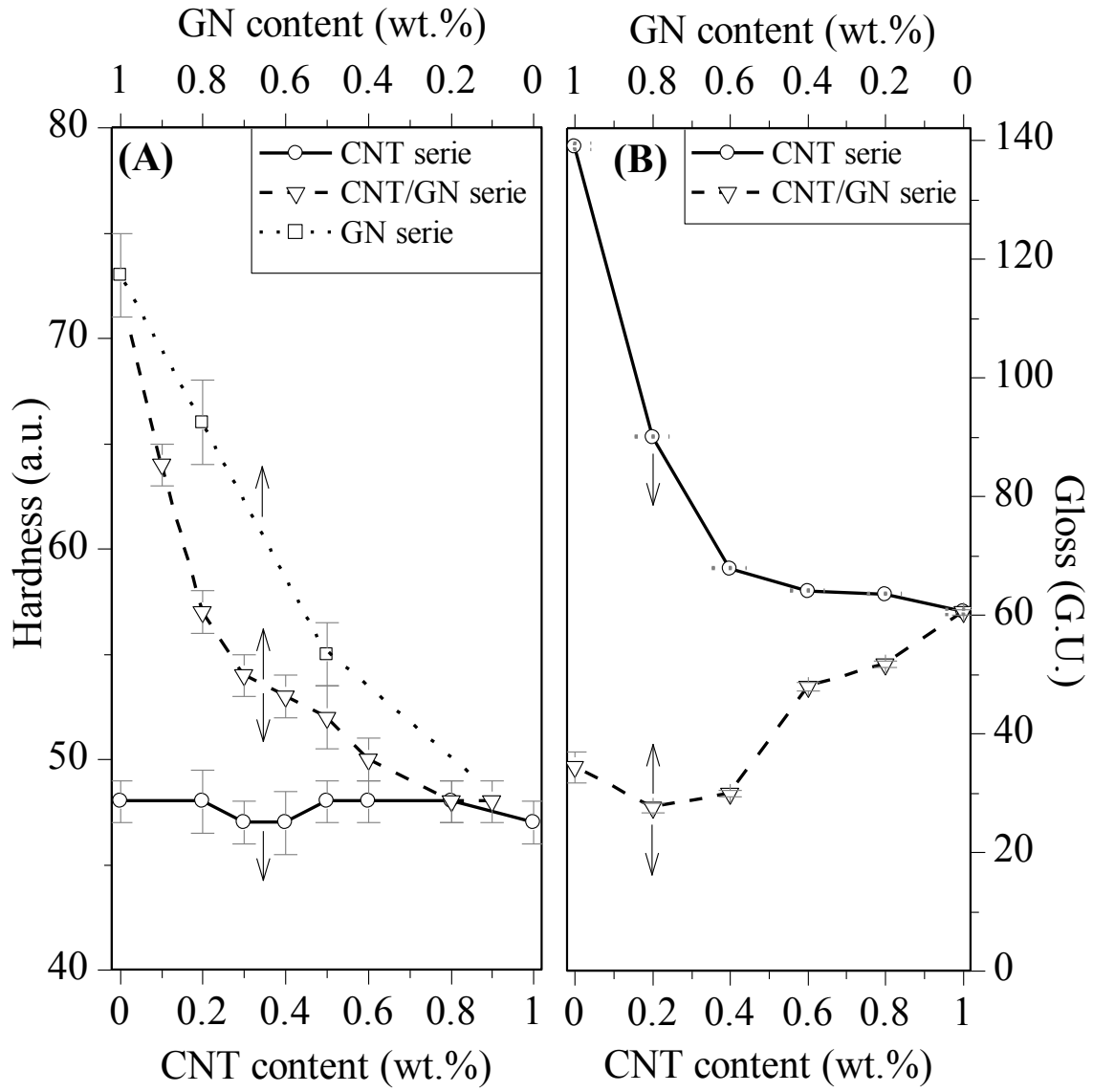


Fig. 4. Hardness (A) and gloss (B) of acrylic coats with carbon nanofillers

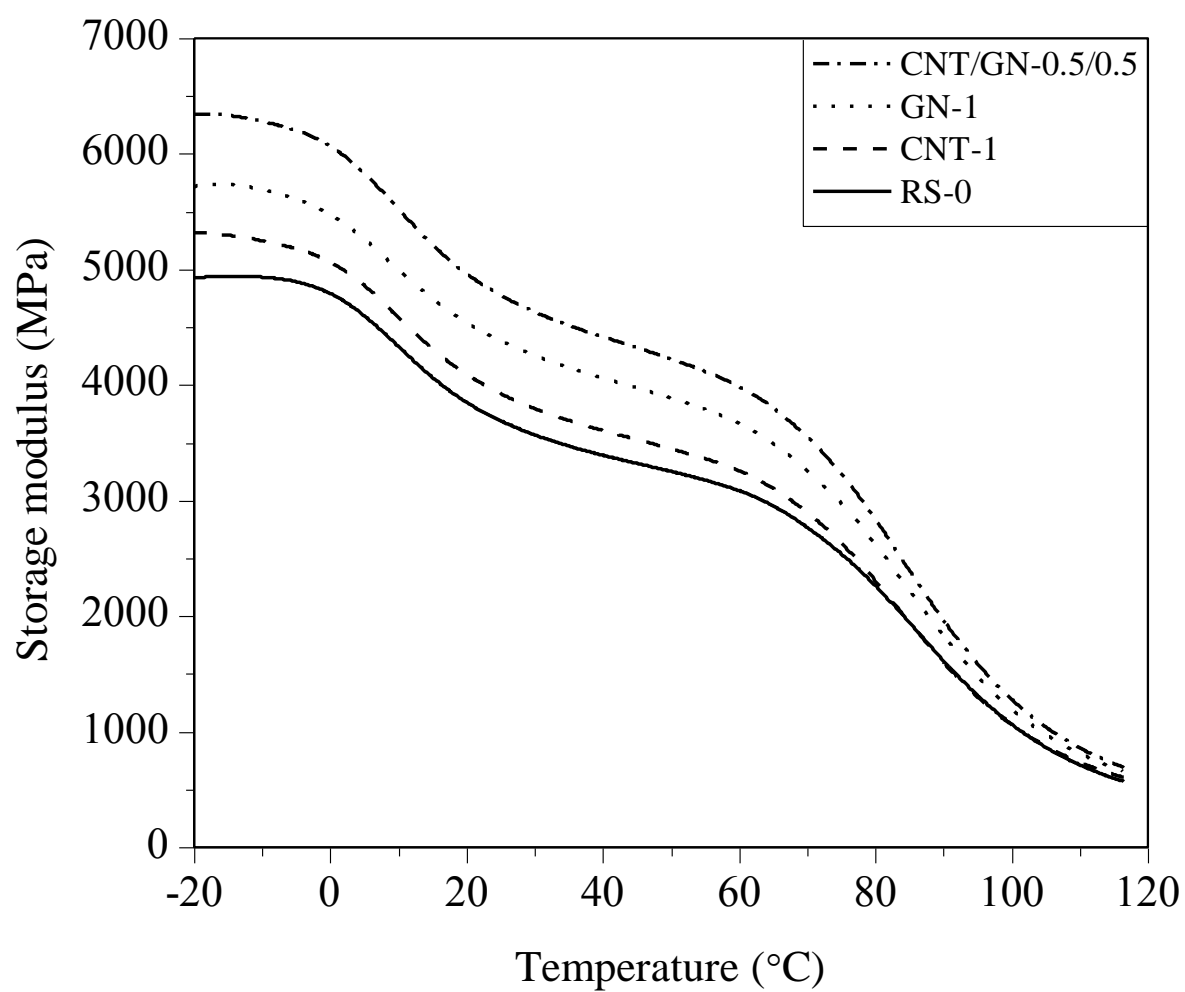


Fig. 5. Storage modulus curves for acrylic coats with carbon nanofillers

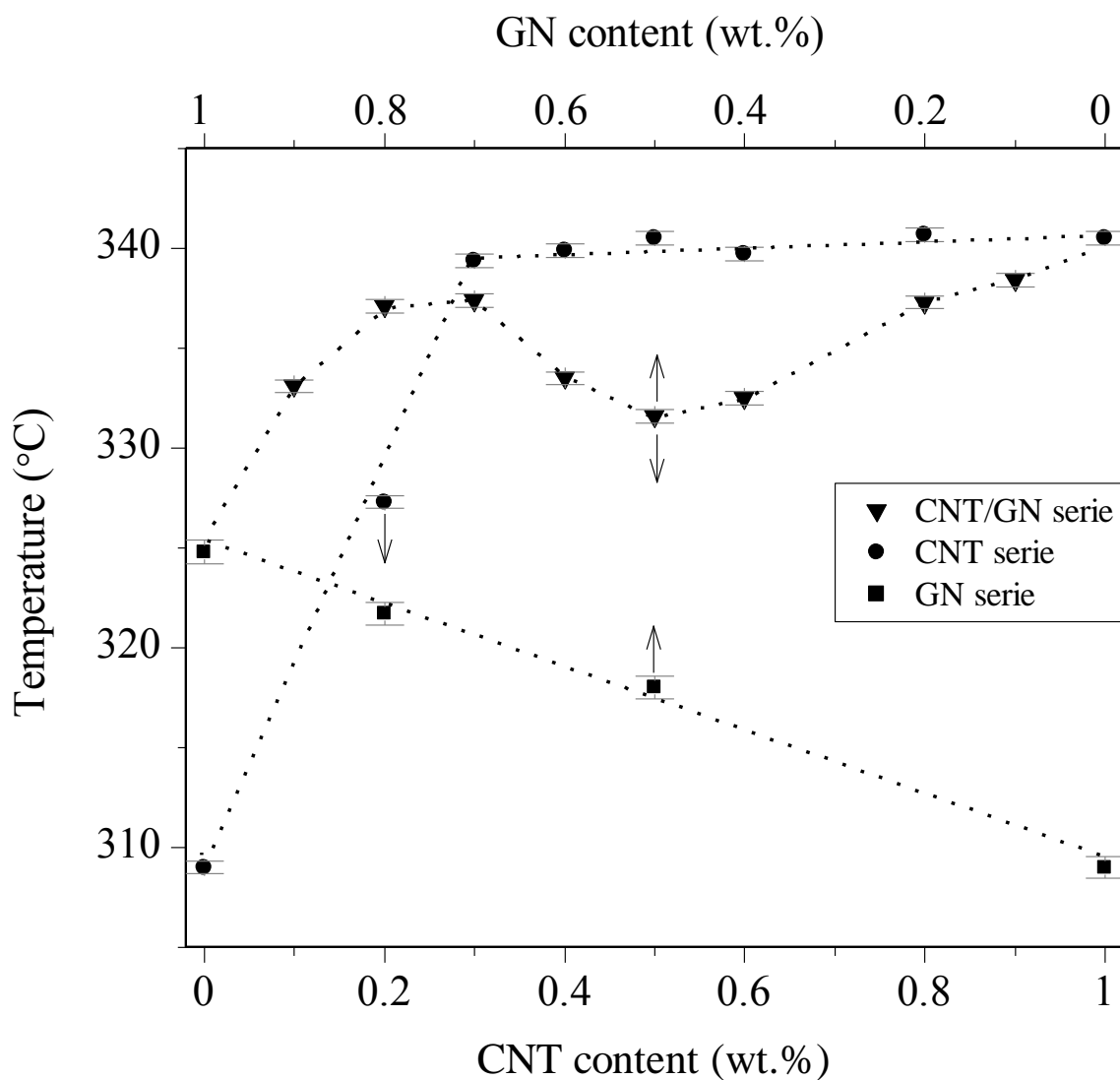


Fig. 6. Temperature at 10 % mass loss (T_{10}) for acrylic coats with carbon nanofillers

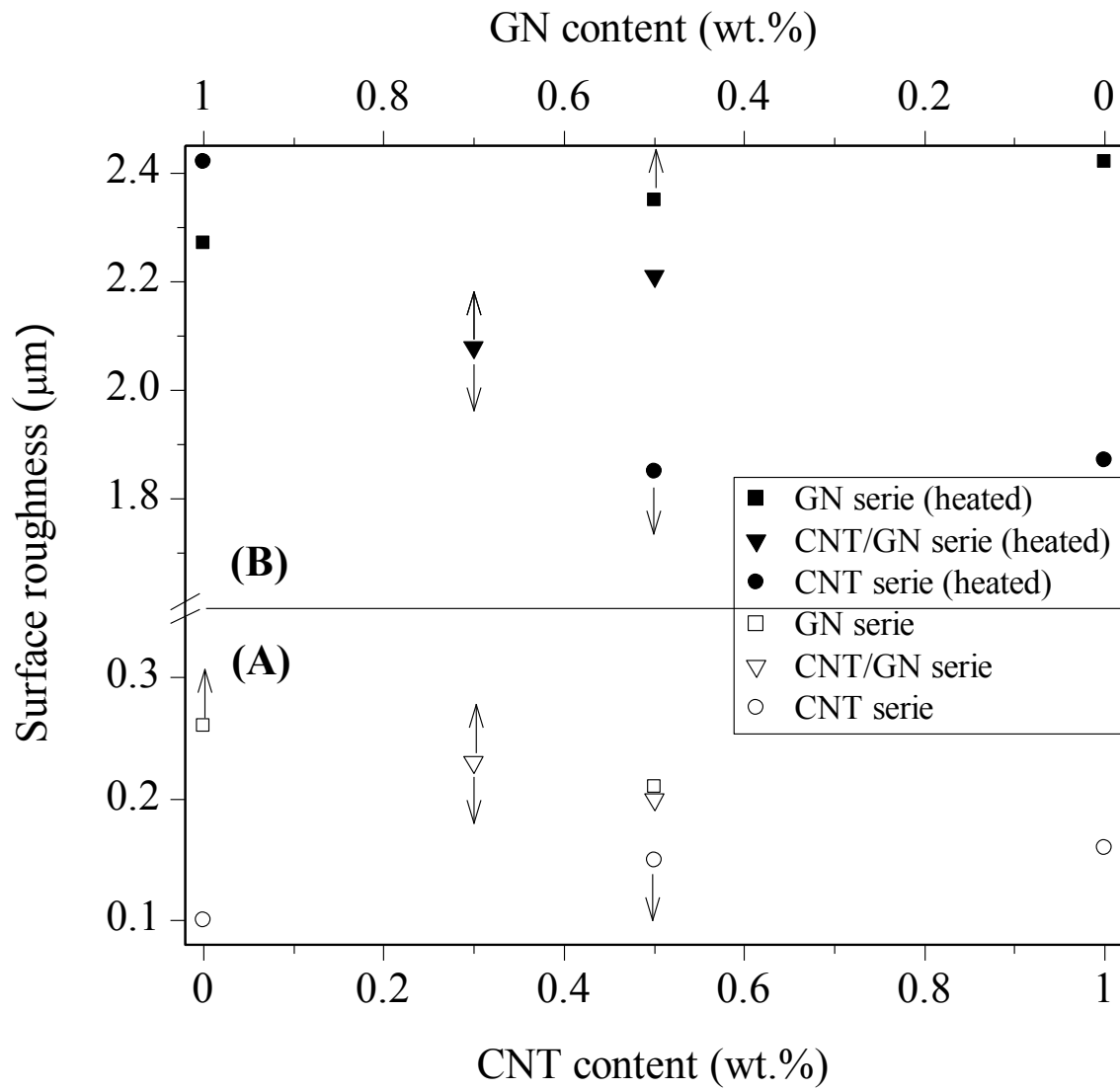


Fig. 7. Surface roughness of acrylic coats with carbon nanofillers (A) before and (B) after heating at 300°C for 0.5 h

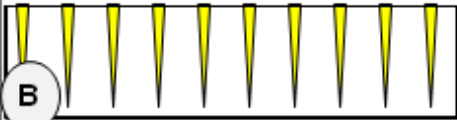
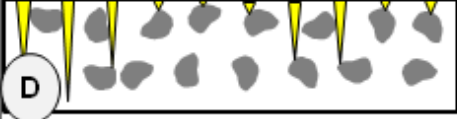
CNs type and content (wt.%)	Dry coat structure	Dry coat structure after 0.5 h at 300 °C
0		
GN: 1		
CNT: 0.25 GN: 0.75		
CNT: 0.5 GN: 0.5		
CNT: 0.75 GN: 0.25		
CNT: 1		
		

Fig. 8. Scheme of the influence of CNs on thermal stability of acrylic coat